Collisions induced by halo and weakly bound nuclei around the Coulomb barrier: experimental results at INFN-LNS

2014 J. Phys.: Conf. Ser. 515 012005

(http://iopscience.iop.org/1742-6596/515/1/012005)

Collisions induced by halo and weakly bound nuclei around the Coulomb barrier: experimental results at INFN-LNS

P. Figuera
INFN Laboratori Nazionali del Sud, Catania, Italy

E-Mail: figuera@lns.infn.it

Abstract. The study of nuclear collisions involving halo or weakly bound nuclei, at energies around the Coulomb barrier, had a considerable interest in the last decade since the peculiar structure of such nuclei can deeply affect the reaction dynamics. In this paper will summarize some of the experimental results obtained by our group at INFN-LNS over the last years in collisions induced by the halo nuclei ^{6}He and ^{11}Be and the stable weakly bound nuclei ^{6}Li and ^{7}Li. Very strong entrance channel effects have been observed in elastic scattering, fusion and direct processes comparing collision induced by the ^{6}He and ^{11}Be halo nuclei with the ones induced on the same target by their cores ^{4}He and ^{10}Be. Collisions induced by the stable weakly bound nuclei ^{6}Li, ^{7}Li shows some peculiarities in comparison to the ones induced by well bound nuclei, such as absence of usual threshold anomaly in the optical potential and strong competition of complete fusion with incomplete fusion and transfer in the heavy residue production cross sections. Our experimental results are compared with the ones of other authors, in order to give an overview of our present understanding of the discussed topic.

1. Introduction

The study of nuclear collisions around the Coulomb barrier induced by halo and, more in general, weakly bound nuclei such as the stable ^{6}Li, ^{7}Li, ^{9}Be, has been the object of many publications in the last decade. In fact, it has been shown that the very low breakup threshold of such nuclei combined with the halo or cluster structure of the ground state, can strongly affect the reaction dynamics around the Coulomb barrier. [e.g. 1-3].

One expects that, direct reaction processes such as breakup or transfer can be favoured by the low breakup threshold coupled with the cluster or halo structure of the ground state. In addition, since the continuum of such nuclei is very close to the ground state, coupling to continuum effects become important both for elastic and the different reaction channels, and a complete theoretical description of such collisions requires complex Continuum Discretized Coupled Channels (CDCC) calculations.

Fusion excitation functions may be affected by static and dynamic effects. Static effects are due to the fact that the diffuse surface of these nuclei affects the shape of the projectile-target potential reducing the average Coulomb barrier, thus leading to a possible enhancement of the fusion cross section. Dynamic effects on fusion, due to the coupling of the different reaction channels, present here a new aspect due to the effects of coupling to continuum. Moreover, fusion reactions in collisions induced by weakly bound nuclei are complicated by the fact that, owing to the large breakup probability, in addition to complete fusion (CF) one can have a non negligible contribution of incomplete fusion (ICF) following breakup of the projectile.

In the last decade our group at INFN-LNS Catania performed different experiments to investigate on the above discussed topics [e.g. 4-12]. In the following, our experimental results will be summarized and compared to the ones of other authors in order to give and overview on what has been observed in such studies, underlining the need of new better quality data for a deeper understanding of the discussed topic.

2. Elastic scattering and direct reactions with halo nuclei: the ^{6}He and ^{11}Be on ^{64}Zn cases

Elastic scattering with halo nuclei around the Coulomb barrier has been measured by different authors on a wide range of target masses. Most of the data are relative to ^{6}He scattering, since this beam has been available for long time at different facilities, with reasonable currents. ^{6}He+^{208}Pb scattering was measured at different energies around the barrier [13,14], and showed a suppression in the region of the Coulomb nuclear interference peak when compared with alpha scattering at the same energy, indicating the presence of long range absorption for ^{6}He. Optical Model (OM) analysis allowed to reproduce the data only using very large imaginary diffuseness. Similar results were observed for ^{6}He scattering on other heavy targets such as for instance ^{197}Au [15]. The ^{6}He scattering data on ^{208}Pb and ^{197}Au were also reproduced within the CDCC approach in [13,16]. ^{11}Li+^{208}Pb elastic scattering around the Coulomb barrier was reported in [17] and compared with the scattering of the ^{11}Li core ^{9}Li on the same target. A huge suppression of the ^{11}Li elastic angular distribution with respect to the ^{9}Li one, much larger than the one observed for ^{6}He, was found. CDCC calculations confirm that, also for this system, coupling to continuum via the Coulomb dipole interaction gives an important contribution to the disappearance of the Coulomb nuclear interference peak. Very few experiments have been performed concerning elastic scattering of halo nuclei on medium mass targets.

At the radioactive beam facility of Louvain la Neuve we measured elastic scattering and direct reactions for collisions induced by the 2n halo nucleus ^{6}He ($S_{2n} \approx 0.9$ MeV), and its core ^{4}He at different energies around the Coulomb barrier [e.g. 4,5]. Some corresponding experimental results are summarized in figure 1. Light particle energy spectra for the ^{6}He induced collision show a large yield of α particles coming from transfer an breakup, which are not observed in the ^{4}He induced collision. The elastic scattering angular distribution for ^{6}He is suppressed when compared to the one for ^{4}He at the same E_{cm}, although the Coulomb nuclear interference pattern is not as much reduced as it was observed for heavy targets. As a consequence, the total reaction cross section for ^{6}He is much larger (about a factor two) than the one for ^{4}He at the same E_{cm} energy. The angular distribution for the large α particle yield observed with ^{6}He is strongly peaked and very different than the one expected for evaporated α particles, confirming that these α particles are produced in transfer and breakup processes. The corresponding transfer and breakup integrated cross section is saturating about 80% of the total reaction cross section, a result which is very different to what observed in collisions induced by well bound nuclei. Similar results have been observed at all measured energies. Our ^{6}He scattering data were reproduced within the CDCC approach [e.g. 16] confirming the importance of coupling to continuum effects.

In the following years we measured, at the REX-ISOLDE facility of CERN, scattering and direct reactions for collisions induced by the 1n halo nucleus ^{11}Be ($S_{n} \approx 0.5$ MeV) and its core ^{10}Be at the same center of mass energy $E_{cm} = 24.5$ MeV [8,9]. As shown in figure 2(a), a suppression of the elastic angular distribution in the region of the Coulomb nuclear interference peak, much stronger than the one observed for ^{6}He on the same target, was found for ^{11}Be. The ^{11}Be elastic scattering angular distribution has been reproduced within the OM, using as bare potential the one that reproduces ^{10}Be scattering, and adding a phenomenological Dynamic Polarization Potential (DPP) having the shape of a Woods-Saxon derivative. A good fit was obtained with a DPP having a large diffuseness of the order of 3.5 fm in agreement with [18]. As shown in figure 2(b), the ^{11}Be data were also reproduced within the CDCC frame, showing that the suppression of the Coulomb nuclear interference peak is due to the combined effect of Coulomb and nuclear couplings to continuum.

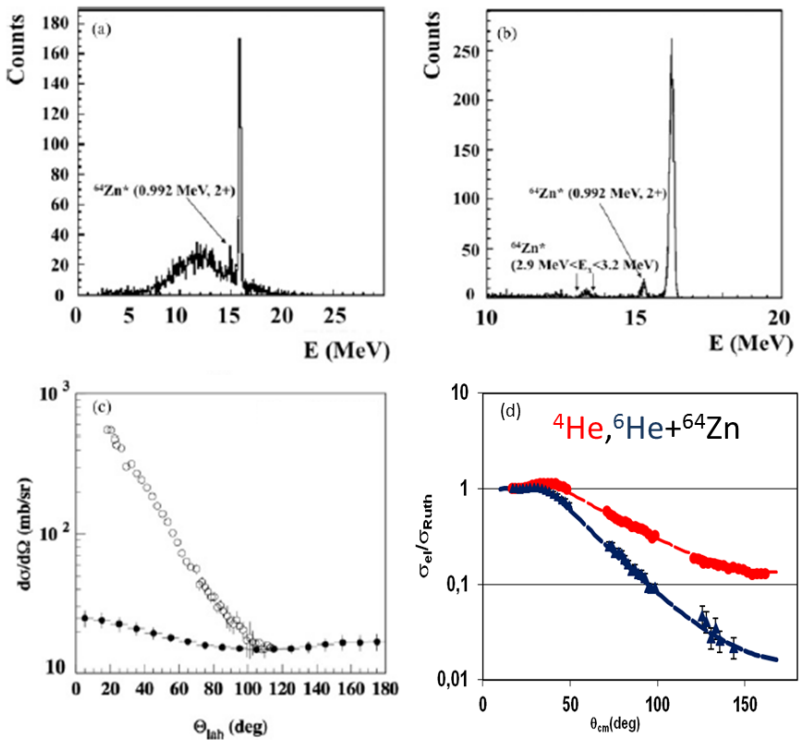

Figure 1. (Color online) (a) Light charged particle energy spectrum for ^{6}He+^{64}Zn at $\theta_{lab}=63^0$ and E_{lab}= 18 MeV. (b) Same as (a) but for ^{4}He+^{64}Zn. (c) Experimental α particle angular distribution at E_{lab}= 18 MeV (open symbols) compared with the one for evaporated α, calculated within the statistical model. (d) Elastic scattering angular distributions for the collisions ^{6}He+^{64}Zn (blue triangles) and ^{4}He+^{64}Zn (red circles) at the same E_{cm} = 12.4 MeV.

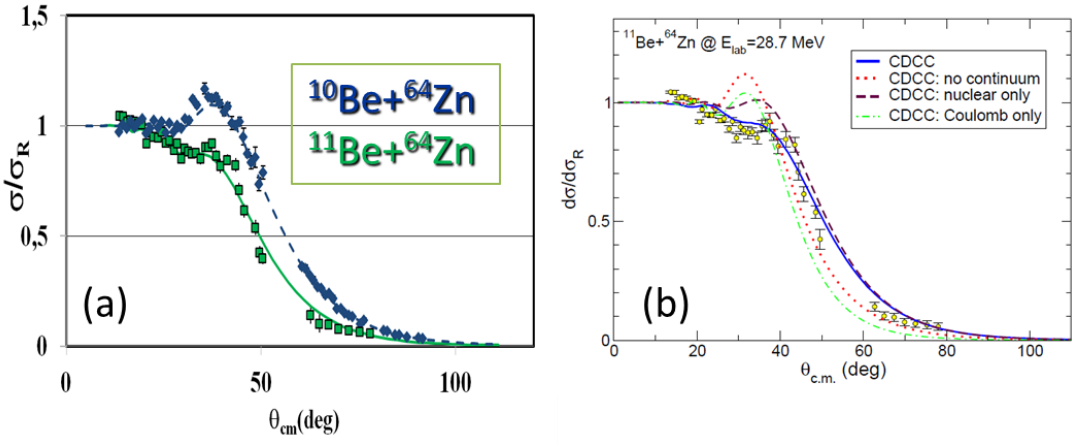

Figure 2. (Color online) (a) Elastic scattering angular distributions for the collisions ^{11}Be+^{64}Zn (green squares) and ^{10}Be+^{64}Zn (blue diamonds) at the same E_{cm}. The continuous lines are the optical model fits. (b) Experimental elastic scattering angular distributions for ^{11}Be+^{64}Zn (symbols) compared with different CDCC calculations.

The total reaction cross section for the collision induced by ^{11}Be is more than a factor two larger than the one for ^{10}Be at the same $E_{cm.}$ In the ^{11}Be+^{64}Zn collision we measured a large yield of ^{10}Be nuclei

produced in transfer and breakup, saturating a large fraction of the total reaction cross section. Although presently available results concerning scattering of halo nuclei around the Coulomb barrier start to show some common features, most of available data are with ^{6}He beams and, in some cases, the results are limited by poor beam quality. Therefore, additional data with different good quality beams, including p-halo ones, are needed to build a wider systematics and allow a deeper understanding of the discussed topic.

3. Fusion reactions with halo nuclei: the ^{4,6}He+^{64}Zn case

Different papers have been published in the literature concerning fusion studies around the Coulomb barrier in collision induced by halo nuclei [e.g. 19-22]. In the last years we measured, in two independent experiments performed at the radioactive beam facility of Louvain La Neuve, the fusion excitation functions around the Coulomb barrier for the systems ^{4,6}He+^{64}Zn [5,6]. The excitation functions have been measured by using an activation technique and all experimental details are reported in [5,6]. Different ^{64}Zn targets followed by Nb catchers were irradiated with ^{4}He beams having energies in the range 8÷10 MeV. The Evaporation Residues (ER) produced in the reaction decay by electron capture (EC) and are implanted in the irradiated target and following catcher. After the end of the activation, we were looking off line at the atomic X rays following the electron capture decay of the residues. This technique allows to charge identify the ER via their characteristic X ray energy. Moreover, following the decay of the targets for a long time, the contribution of the different isotopes can be separated due to their different half lives, allowing a complete mass and charge identification.

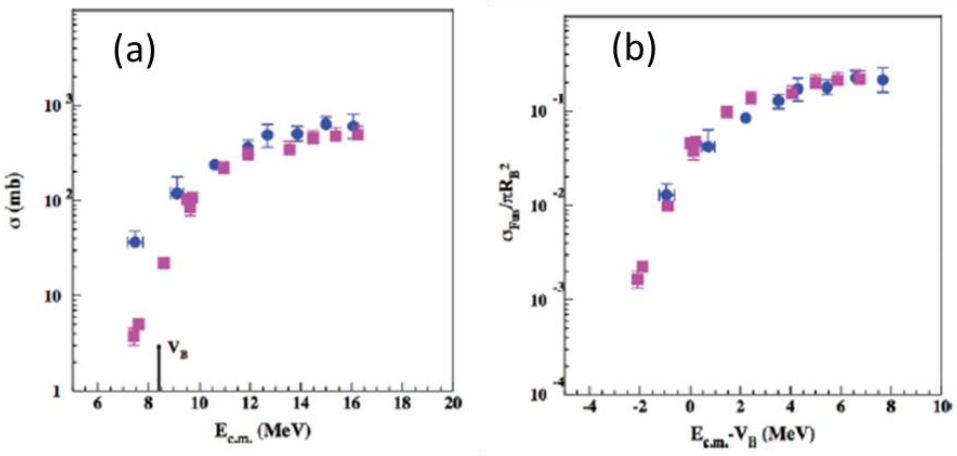

Figure 3. (Color online) (a) Fusion excitation functions for ^{6}He+^{64}Zn (blue circles) and ^{4}He+^{64}Zn (purple squares). The arrow indicates the position of the Coulomb barrier. (b) Reduced fusion excitation functions for ^{6}He+^{64}Zn (blue circles) and ^{4}He+^{64}Zn (purple squares) to eliminate static effects. See text for details.

In Figure 3(a) the ^{6}He+^{64}Zn fusion excitation function is compared with the one for ^{4}He+^{64}Zn. As one can see, an enhancement of fusion for the collision induced by the halo nucleus ^{6}He is observed in the region around the barrier ($V_B \approx 9$MeV). As discussed in the introduction, fusion enhancement effects in collisions induced by halo nuclei may be due to a combination of static and dynamic effects. Static effects, due to the extended matter distribution in ^{6}He, can be removed by comparing reduced fusion excitation functions i.e. ($\sigma/\pi R_B^2$) versus (E_{cm}-V_B) were V_B and R_B are the barrier and barrier radius extracted from potentials calculated with realistic densities [23]. As shown in figure 3(b), by performing such comparison, the observed enhancement disappears and we therefore conclude that it

can be explained as mainly due to static effects. Enhancement of fusion cross section around the barrier in collisions induced by halo nuclei, with respect to collisions induced by the halo nucleus core, has been found for different systems in the literature [e.g. 6, 21-23]. Recently, a consistent systematic comparison of many published fusion data, in collisions induced by halo and weakly bound nuclei on targets of different mass, was published [e.g. 23-25]. Such systematic study suggests that, for collisions induced by halo nuclei, once static effects are removed, the residual effect of coupling to continuum or transfer is a suppression of fusion above barrier and, most probably, a residual enhancement of fusion below the barrier. Unfortunately most of presently available data do not explore the sub-barrier region with reasonable errors and new data would be necessary for a complete understanding of this topic. This, however, is very difficult due to the low intensities of halo nuclei beams presently available.

4. Elastic scattering of ^{6,7}Li+^{64}Zn and threshold anomaly in the Optical Potential

The study of collisions induced by stable weakly bound nuclei such as ^{6}Li(S_α=1.47 MeV), ^{7}Li(S_α=2.47 MeV) and ^{9}Be(S_n=1.66 MeV), which do not have a halo structure, has also a considerable interest to investigate on the problems discussed in the introduction. When compared with halo nuclei, they have larger breakup threshold and do not show the same extended mass distribution. However, coupling to continuum effects with such nuclei are still expected to be important and, since beams of such stable nuclei are available with high currents, high quality data can be collected.

One of the problems which has been investigated in the literature concerns the energy dependence of the optical potential in collisions induced by such nuclei. It is well known that the optical potential extracted by the analysis of the elastic scattering of heavy ions, involving tightly bound nuclei, shows a variation with energy in the region of the Coulomb barrier, a phenomenon known as the threshold anomaly (TA) (see, e.g. [26]). The strength of the imaginary potential decreases sharply as the incident energy decreases toward the Coulomb barrier energy, while the real part of the potential increases and shows a bell-shaped peak in the same energy region. The TA has been ascribed to the energy dependence of the dynamic polarization potential that originates from the coupling of the elastic scattering to the non-elastic channels. The coupling to non-elastic channels results in an attractive real polarization potential. The decrease of the imaginary potential can be understood as due to the closure of non-elastic channels at energies near and below the Coulomb barrier.

Recently, much work has been devoted to the study of the TA in elastic scattering of weakly bound nuclei, such as ^{6}Li and ^{7}Li. For these projectiles the breakup channel is expected to be important even at energies below the Coulomb barrier. The coupling to the breakup produces a repulsive polarization potential [e.g. 27] and, therefore the usual TA in the OP may disappear.

In order to investigate on this topic, we measured elastic scattering angular distributions at several energies around the barrier for the systems ^{6,7}Li+^{64}Zn. The measurements have been performed at the Catania tandem by using an array of five ΔE(10 μm)-E(200 μm) telescopes mounted on a rotating arm, in order to measure the angular distributions in a wide angular range. As an example, the elastic angular distributions for the system ^{6}Li+^{64}Zn are shown in figure 4. As one can see, at energies below the Coulomb barrier (V_B ~13 MeV in the present system) the difference between the elastic and the Rutherford cross sections is rather small, therefore good quality data are needed to perform such investigations. The experimental angular distributions have been reproduced via optical model fits using a renormalized optical potential both for the real and imaginary part, leaving the renormalization coefficients as free parameters. As an example, the obtained trend of the renormalization coefficients for the ^{6}Li+^{64}Zn case is shown in figure 5 . As one can see, the data show a rather 'flat' behaviour around the Coulomb barrier corresponding to a clear absence of the usual threshold anomaly. Similar conclusions were obtained using a Woods-Saxon imaginary potential. We found Similar results also for the ^{7}Li+^{64}Zn system. Details of the used experimental procedure are reported in [11]. Absence of the usual threshold anomaly in the OP, in collisions induced by weakly bound nuclei both stable and radioactive has been observed by many other authors in the literature [e.g. 28-32]

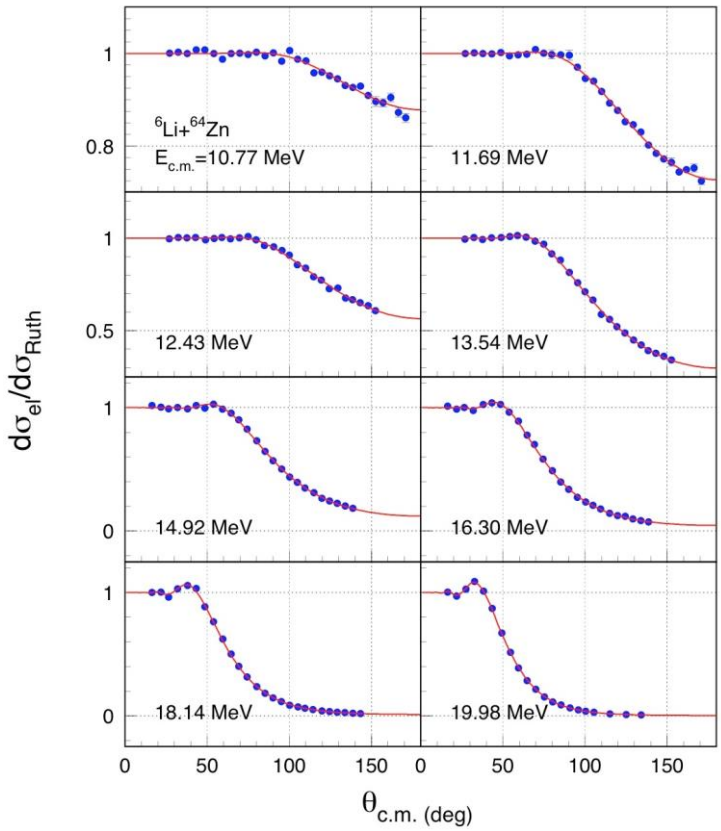

Figure 4. (Color online) Elastic scattering angular distributions measured for the system ^{6}Li+^{64}Zn. The continuous lines are the results of the optical model fits.

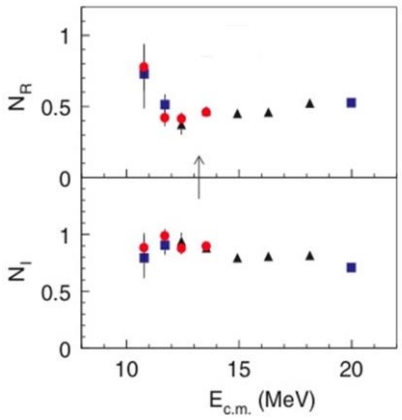

Figure 5. (Color online) Renormalization coefficients for the real and imaginary part of the potential in the collision ^{6}Li+^{64}Zn. The position of the Coulomb barrier is indicated by the arrow. Different symbols refer to independent experiments.

5. Fusion excitation functions with stable weakly bound nuclei: the ^{6,7}Li+^{64}Zn case

Fusion excitation functions in collisions induced by stable weakly bound nuclei have been measured for several systems in a wide target mass range [e.g. 33-40]. For fusion-evaporation reactions induced by weakly bound nuclei on heavy targets [e.g. 33-36], where the emission of charged particles is

hindered by the presence of a strong Coulomb barrier, the CF and ICF contributions can be usually clearly separated since they produce evaporation residues (ER) having different charge. The main finding for such systems is that CF is suppressed above the barrier by about 30% with respect to the prediction of Single Barrier Penetration (SBP) calculations or Coupled Channel (CC) calculations not taking into account coupling to continuum. Since the sum of CF and ICF, normally referred as total fusion (TF), is not suppressed, it was suggested that the observed suppression is mainly due to breakup of the projectiles followed by ICF.

For fusion of weakly bound nuclei on medium mass or light targets [e.g. 37-40], the compound nucleus can evaporate charged particles. Therefore, the same residues can be populated by the CF and ICF mechanisms, making their separation much more difficult. For this reason, most of the fusion data for light and medium mass systems are relative to TF cross section which, as for collisions on heavy targets, do not show any suppression or enhancement effect above barrier, whereas below the barrier not much data are available.

Recently we measured excitation functions for heavy residue (HR) production in the collisions ^{6,7}Li+^{64}Zn around the Coulomb barrier, with the aim to extract some information on the competition between CF, ICF and other reaction mechanisms in the HR production. The experiment has been performed at the Catania tandem with the same activation technique mentioned in section 3 and all the experimental details are reported in [10]. Excitation functions for HR production are shown in figure 6, together with the results of SBP calculations and CC calculations including the excitation of different states of projectile and target. As one can see, both calculations reproduce the data above barrier but fail below it. In order to understand which are the possible reaction mechanisms responsible for heavy residue production, the experimental relative yield of the HR was compared with different statistical model calculations performed using the code Cascade.

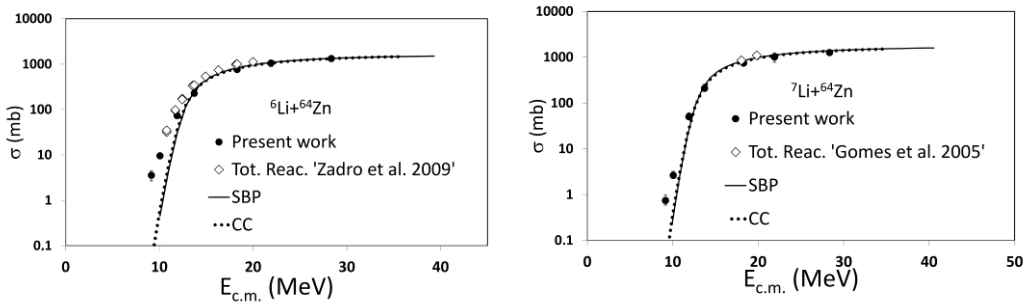

Figure 6. Excitation functions for heavy residue production (full circles) and total reaction (open diamonds) for the systems ^{6}Li+^{64}Zn and ^{7}Li+^{64}Zn. The total reaction data are from refs. [11,37].

Since ^{6}Li and ^{7}Li have weakly bound cluster structures of the ground state with separation energies S_α=1.47 and S_α=2.47 MeV respectively, we expect reactions where only an alpha particle, a deuteron or a tritium are captured by the target. This may happen in two different ways, breakup followed by incomplete fusion (ICF) or a direct cluster transfer (DCT). Since ICF and DCT populate the same nuclei with similar excitation energies, we cannot distinguish between the two modes in the present experiments. Expected relative yields of the HR populated in ICF or DCT have been calculated with Cascade. The excitation energies following the d, t or α capture were estimated assuming an ICF mechanism where the available fragment-target centre of mass energy before ICF occurs is: $(E_{c.m.}-S_\alpha)\times(m_{clu}/m_{proj})$. Here $E_{c.m.}$ is the initial centre of mass energy of the Li+^{64}Zn system, S_α is the α separation energy of the projectile and m_{clu} and m_{proj} are the masses of the captured cluster and of the projectile respectively. Excitation energies estimated for DCT were only slightly smaller than the ones for ICF, giving basically the same relative yield as for ICF. A comparison between the expe at

two different energies. As one can see, above the Coulomb barrier (V_B ~ 13 MeV), the experimental relative yields are similar to the ones predicted by CF Cascade calculations, showing that CF is the dominating mechanism. However, at energies below the barrier, the HR experimental relative yield is rather different than the one expected for CF, showing that CF is no longer the dominating reaction mechanisms while other processes such as ICF, DCT or single nucleon transfer become very important. As one can see in figure 7, for ^{6}Li+^{64}Zn the relative yield below the barrier is dominated by ^{65}Zn and ^{65}Ga which are not expected in CF but can be produced in ICF/DCT of a deuteron as well as in 1n and 1p transfer reactions respectively. Similar results were also observed for ^{7}Li+^{64}Zn. Present results suggest therefore that, in order to study fusion below the barrier in collisions induced by weakly bound nuclei on medium mass targets, the simple integration of the HR yield is not giving us the TF cross sections since different processes such as DCT and single neutron transfer can give an important contribution. Therefore, one needs to find experimental techniques allowing to properly separate the different reaction mechanisms contributing to the HR yield.

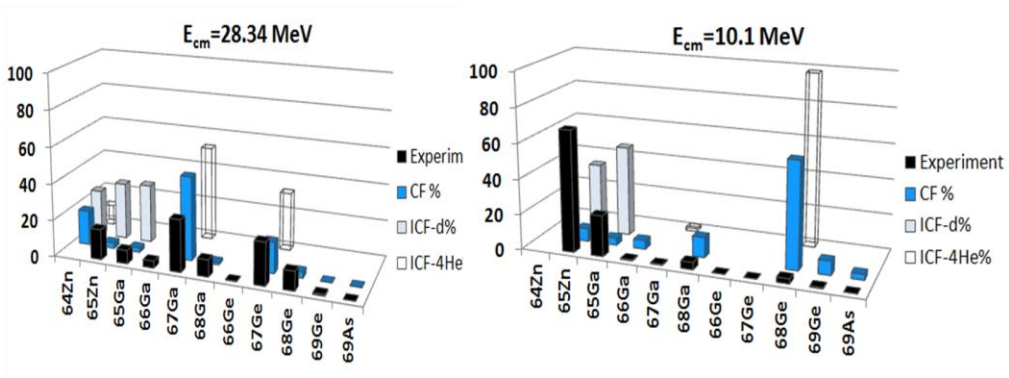

Figure 7. (Color online) Experimental heavy residue relative yield for ^{6}Li+^{64}Zn compared with the prediction of statistical model calculations for complete fusion and deuteron or α capture.

6. Summary and conclusions

In this paper our experimental results, concerning the study of elastic scattering and reactions for halo and stable weakly bound nuclei around the Coulomb barrier on a ^{64}Zn target, have been summarized and compared with the ones of other authors.

We have shown that, in collisions induced by halo nuclei, a strong suppression of the elastic scattering cross section and, correspondingly, a large enhancement of the total reaction cross section has been observed by various authors. It has been found that the observed enhancement of the total reaction cross section is due to a very large yield of transfer and breakup which, contrary to what observed with well bound projectiles, saturates most of the total reaction cross section. In particular, in collisions induced by the 2n halo nucleus ^{6}He, it has been found that the 2n transfer process is the most important reaction channel around the Coulomb barrier. In order to reproduce the measured elastic scattering angular distributions within the OM, one has to use rather large diffuseness of the imaginary part showing the presence of long range absorption. Elastic scattering data have also been reproduced by different authors within the CDCC frame showing that the measured elastic scattering angular distributions cannot be reproduced without taking into account coupling to continuum effects.

Fusion excitation functions in collisions induced by halo nuclei have also been measured by different authors. Presently, available results suggest the presence of a fusion cross section enhancement around the barrier for halo nuclei when compared both to SBP calculations based on potentials which do not take into account the diffuse structure the projectile, or to the excitation functions induced by the halo

nucleus core on the same targets. Although most of the observed effect on fusion can be described as due to static effects, these are not the only ones, and it has been suggested that coupling to continuum or transfer channels is also playing an important role.
Elastic scattering and fusion have also been studied in collisions induced by the stable weakly bound nuclei ^{6}Li, ^{7}Li and ^{9}Be, having low breakup thresholds and a marked cluster structure of the ground state. Elastic scattering with such nuclei has been studied by different authors and reproduced with OM fits. For many of the studied systems, including our ^{6,7}Li+^{64}Zn data, the obtained energy dependence of the real and imaginary part of the OP, extracted from the OM fits, show absence of the usual threshold anomaly. This has been interpreted ad due to the presence of a repulsive polarization potential due to coupling to continuum effects. Fusion excitation functions with stable weakly bound nuclei have also been studied. In collision on heavy targets, were CF and ICF can be easily separated, data show a well established suppression of CF due to ICF following projectile breakup. In collisions with medium mass or light targets CF and ICF cannot be easily separated and most of available data refers to TF. Our ^{6,7}Li+^{64}Zn fusion data suggest that above barrier HR production is dominated by CF. Below the barrier, on the contrary, other processes such as ICF but also direct cluster transfer or single neutron transfer are the dominating processes for HR production.
Although different aspects of the discussed topics have been clarified by the papers published so far, new better quality data would be necessary for a more complete understanding to our opinion.
Almost all the results obtained so far for collisions induced by halo nuclei have been obtained with ^{6}He beams and additional data with different halo nuclei would be necessary to build up a compete systematics. At the same time, new fusion cross sections measurements with halo nuclei, better exploring the sub-barrier region are still needed, since most of the data available do not explore this energy range with reasonable errors.
In the study of collisions induced by stable weakly bound nuclei, new fusion cross sections measurements would be needed, especially on medium mass or light targets, at energies extending well below the barrier. These measurements should possibly be performed with experimental techniques allowing to clearly disentangle among the transfer, CF and ICF mechanisms leading to the production of the detected heavy residues, in order to bring new clear information on fusion and competing reaction mechanisms.

Acknowledgments
Our experimental results discussed in the present review paper, have been obtained over the last decade in different experiments involving many colleagues, belonging to INFN-LNS and other institutions, whose contribution is gratefully acknowledged.

References
[1] Canto L F et al. 2006 *Phys. Rep.* **424** 1
[2] Keeley N et al. 2007 *Prog. Part. Nucl. Phys.* **59** 579
[3] Keeley N et al. 2009 *Prog. Part. Nucl. Phys.* **63** 396
[4] Di Pietro A et al. 2003 Euro*phys. Lett.* **64** 309
[5] Di Pietro A et al. 2004 *Phys. Rev. C* **69** 044613
[6] Scuderi V et al. 2011 *Phys. Rev. C* **84** 064604
[7] Di Pietro A et al. 2007 *Eur. Phys. J. Spec. Top.* **150** 15
[8] Di Pietro A et al. 2010 *Phys. Rev. Lett.* **105** 022701
[9] Di Pietro A et al. 2012 *Phys. Rev. C* **85** 054607
[10] Di Pietro A et al. 2013 *Phys. Rev. C* **87** 064614
[11] Zadro M et al. 2009 *Phys. Rev. C* **80** 064610
[12] Zadro M et al. 2013 *Phys. Rev. C* **87** 054606
[13] Acosta L et al. 2011 *Phys. Rev. C* **84** 044604
[14] Sanchez Benitez A M et al. 2008 *Nucl. Phys. A* **803** 30
[15] Kakuee O R et al. 2006 *Nucl. Phys. A* **765** 294

[16] Moro A M et al. 2007 *Phys. Rev. C* **75** 064607
[17] Cubrero M et al. 2012 *Phys. Rev. Lett.* **109** 262701
[18] Bonaccorso A et al. 2002 *Nucl. Phys. A* **706** 322
[19] Raabe R et al. 2004 *Nature* **431** 823
[20] Kolata J J et al. 1998 *Phys. Rev. Lett.* **81** 4580
[21] Lemasson A et al. 2009 *Phys. Rev. Lett.* **103** 232701
[22] Alcorta M et al. 2011 *Phys. Rev. Lett.* **106** 172701
[23] Canto L F et al. 2009 *Nucl. Phys. A* **821** 51
[24] Rangel J et al. 2013 *Eur. Phys. Jour. A* **49** 57
[25] Gomes P R S et al. 2009 *Phys. Rev. C* **79** 027606
[26] Satchler G R et al. 1991 *Phys. Rep.* **199** 147
[27] Sakuragi Y et al. 1987 *Phys. Rev. C* **35** 2161
[28] Maciel A M M et al. 1999 *Phys. Rev. C* **59** 2103
[29] Pakou A et al. 2004 *Phys. Rev. C* **69** 054602
[30] Kumawat H et al. 2008 *Phys. Rev. C* **78** 044617
[31] Figueira J M et al. 2010 *Phys. Rev. C* **81** 024613
[32] Deshmukh N N et al. 2011 *Phys. Rev. C* **83** 024607
[33] Dasgupta M et al. 2004 *Phys. Rev. C* **70** 024606
[34] Gomes P R S et al. 2006 *Phys. Rev. C* **73** 064606
[35] Wu Y W et al. 2003 *Phys. Rev. C* **68** 044605
[36] Pradhan M K et al. 2011 *Phys. Rev. C* **83** 064606
[37] Gomes P R S et al. 2005 *Phys. Rev. C* **71** 034608
[38] Anjos R M et al. 2002 *Phys. Lett. B* **534** 45
[39] Sinha M et al. 2010 *Eur. Phys. J. A* **44** 403
[40] Beck C et al. 2003 *Phys. Rev. C* **67** 054602